Microwave Absorbing Properties of DBSA-doped Polyaniline/BaTiO$_3$-Ni$_{0.5}$Zn$_{0.5}$Fe$_2$O$_4$ Nanocomposites

Prof. Chapal Kumar Das (Corresponding author)

Materials Science Centre, Indian Institute of Technology-Kharagpur

Kharagpur- 721302, West Bengal, India

Tel: 91-322-028-3978   E-mail: chapal12@yahoo.co.in

Avinandan Mandal

Materials Science centre, Indian Institute of technology, Kharagpur

Kharagpur- 721302, West Bengal, India

Tel: 91-964-122-7589   E-mail: avinandanmandal@gmail.com

Abstract

Development of RADAR absorbing materials (RAMs) is the most important research area in camouflage application mainly in Defence. Aniline was polymerized in presence of dodecylbenzene sulphonic acid (DBSA) as a functionalized protonic acid in water medium to form DBSA-doped polyaniline (PANI). Ni$_{0.5}$Zn$_{0.5}$Fe$_2$O$_4$ (NZF) nanoparticles were synthesized by co-precipitation method along with Bariun Titanate (BaTiO$_3$) particles to form BaTiO$_3$-Ni$_{0.5}$Zn$_{0.5}$Fe$_2$O$_4$ nanoparticles. Both DBSA-doped PANI and BaTiO$_3$-Ni$_{0.5}$Zn$_{0.5}$Fe$_2$O$_4$ nanoparticles were thoroughly mixed in different ratios and the mixtures were dispersed in Epoxy Resin (LY556) matrices to produce RAMs. The spectroscopic characterization of the composite materials were examined by using X-ray diffraction (XRD), scanning electron microscope (SEM), Energy-dispersive X-ray spectroscopy (EDX), High resolution transmission electron microscopy (HR-TEM). The microwave absorbing properties return loss (dB) and important parameters such as complex relative permittivity (ε_r' - jε_r''), complex relative permeability (μ_r' - jμ_r'') were measured in different microwave frequencies in X-band (8.2-12.4 GHz) region. The composite materials showed that a wider absorption frequency range and showed maximum return loss of -15.78 dB (>97% power absorption) at 10.8 GHz. The mechanism of microwave absorption occurs mainly due to the dielectric loss rather than magnetic loss.

1. Introduction

Development of RADAR absorbing material started in 1930s but commercial production started in 1950s. Radar absorbing materials (RAMs) are widely used in commercial as well as military applications (Wen et al., 2008; John et al., 1988). Microwaves have two components, electric field and magnetic field perpendicular to each other. So it is required to cancel out both the component to get effective absorption when materials will be exposed to Microwave i.e. reduction of Radar Cross Section (RCS). The RAMs are prepared with the compounds having high loss energy. The excellent RAMs show the microwave absorbing properties over a wide frequency range and the materials should be lightweight and thin. From the literature survey, it has been concluded that the various types of absorbers such as ferroelectric (Chen et al., 2007) and ferromagnetic materials (Maeda et al., 2004) and also conducting materials (Fan et al., 2006; Wojkiewicz et al., 2003; Soto-Oviedo et al.,2006) are utilized for this purpose. Soft ferromagnetic materials are used as microwave absorbing materials due to their high specific resistance, high magnetic saturation and low coercivity. Soft ferromagnetic materials like spinel ferrites have been utilized as the absorbing materials in various forms. Recently, it has been shown that magnetic nanocomposites are more useful due to their advantage with respect to light weight, design flexibility and better absorbing properties over pure ferrites (Singh et al., 2000). On the other

hand, ferroelectric materials have permanent dipoles. Due to this polarization, microwave absorption occurs. Microwave absorbing properties of Ferromagnetic-conducting polymer (Ting et al., 2011) or ferroelectric-conducting polymer composite (Abbas et al., 2005) materials have been reported by using different types of ferromagnetic and ferroelectric fillers. In the present research work, there is an interest in the use of magneto-electric based absorbing materials that provide absorption over a wide frequency range. Magneto-electric composite materials are established by using both the magnetic and electric media. Magneto-electric composite materials show the magneto-electric effect and electromagnetic properties that are absent in their constituent phases (Burke et al., 2002; Kadam et al., 2005; Fetisov et al., 2004; Kanai et al., 2001). Magneto-electric effects of ferroelectromagnet are the magnetic polarization on applying the electric field or generate electric polarization on applying magnetic field. These effects are due to the interaction between magnetic and electric dipoles (Burke et al., 2002; Kadam et al., 2005). Based on our knowledge, barium titanate ($BaTiO_3$) and $Ni_{0.5}Zn_{0.5}Fe_2O_4$ were utilized as the ferroelectric and ferromagnetic materials respectively. Among the conducting polymers, poly-aniline (PANI) was most widely studied due to its unique properties (Li et al., 2007; Mathur et al., 2001). It has high conductivity, high resistance to air, light weight, low cost, good electrical properties and good processibility (Li et al., 2008; MacDiarmid and Epstein, 1995; Aphesteguy and Jacobo, 2004). It has also used as electromagnetic interference (EMI) shielding, electro-catalyst, rechargeable battery, chemical sensors, and microwave absorption (Moghaddam and Nazari, 2008; Sarac et al., 2008). PANI exhibits better electronic and physical properties in its protonated state and it also shows magnetic properties due to high spin density. PANI was protonated by DBSA to form DBSA-doped PANI (Babazadeh, 2009) and on the other hand $BaTiO_3$-$Ni_{0.5}Zn_{0.5}Fe_2O_4$ particles (magneto-electric materials) were prepared by the co-precipitation method (Testino et al., 2006). Both DBSA-doped PANI and magneto-electric materials were ground to get fine powder of sub-micron size and the powder was thoroughly mixed separately in three different ratios, 3:1, 1:1, and 1:3 respectively. RAMs were developed by dispersing these mixed powder particulates in epoxy resin matrices, keeping the pigment to volume concentration (PVC) constant as ~25% in all the samples. The ferroelectric phase, ferromagnetic phase and conducting phase coexist in one material; magneto-electric properties and the other coupling are expected due to interaction between magnetization and electric polarization. The developed RAMs showed the absorbing properties in a wide frequency range.

2. Experimental Work

2.1 Materials

Aniline (99.5%) was purchased from Sigma-Aldrich and Dodecylbenzene sulphonic acid (DBSA), ammonium per sulfate (APS, 98.5%) were purchased from Merck (India). Nickel nitrate (Ni $(NO_3)_2$, $6H_2O$), zinc nitrate (Zn $(NO_3)_2$, $6H_2O$), ferric nitrate (Fe $(NO_3)_3$, $9H_2O$), barium titanate ($BaTiO_3$) and sodium hydroxide (NaOH) of analytical reagent grade were obtained from Loba chemie (India). All reagents were used without further purification. Distilled water was used in all the experiments.

2.2 Preparation of DBSA-doped PANI

In a 1000 ml-flat bottom flask as a reactor, DBSA (90 mmol) was taken with 400 ml distilled water and aniline (90 mmol) was poured into the flask to form a homogeneous white milky dispersion of anilinium-DBSA complex. The flask was placed into ice-bath containing salt and cooled to 0-5ºC. Then 90 mmol of APS was dissolved in 200 ml of distilled water and added into the flask during 2 min. at the mentioned temperature. After 24 hours, a dark-green suspension of DBSA-doped PANI was precipitated with 500 ml of acetone. This precipitation was filtered and washed several times with distilled water and dried at 60ºC for 48 hours. The formed product was grounded to get powder.

2.3 Preparation of $BaTiO_3$-$Ni_{0.5}Zn_{0.5}Fe_2O_4$

The molar ratio of $BaTiO_3$ and NZF was taken as 1:1. Suitable combination of ferroelectric and ferromagnetic materials would give the better magnetoelectric property. It has been shown by the earlier worker (Testino et al., 2006) that with increasing the concentration of $BaTiO_3$, the magnetic property was decreased for $xBaTiO_3$-$(1-x)$ $Ni_{0.5}Zn_{0.5}Fe_2O_4$ (x= 0.5, 0.6, 0.7) composites. Hence we have used 50% of both $BaTiO_3$ and NZF as the best composition. Due to the equal concentration of both ferroelectric and ferromagnetic materials, there should be better interfacial interaction between them. $BaTiO_3$ particles were dispersed in the NaOH solution by the sonication and vigorous staring. The nitric cation solutions were added quickly to the alkaline solution in the same concentration and the molar ratio of OH/NZF was taken 8. This solution was heated to 100ºC for 1 hr. to complete the reaction. The resulting suspension was washed with water several times and twice with acetone. The powder was recovered by filtration and dried at 60ºC for 12 hr and then this powder was calcined at 900ºC for 1 hr. to form the NZF phase. The product was manually milled to form the fine powder.

2.4 Preparation of Microwave Test Plate

DBSA-doped PANI and $BaTiO_3$-$Ni_{0.5}Zn_{0.5}Fe_2O_4$ nanoparticles were mixed separately in three different ratios, 3:1, 1:1 and 1:3. The prepared mixed powder was dispersed in epoxy resin matrices at 80˚C with the help of mechanical stirrer for 1 hour and cured at 75˚C for 30 minutes. The composite samples were prepared by dispersing these mixed powder particulates in epoxy resin matrices and designated as RAM-I, RAM-II, RAM-III respectively. The pure $BaTiO_3$-$Ni_{0.5}Zn_{0.5}Fe_2O_4$ nanoparticles were dispersed in epoxy resin and designated as RAM-IV. Particulate to binder volume ratio was kept as ~25% in all four samples and thickness of all the samples were taken approximately 2 mm. All the four samples were cut into desired rectangular shape of size 0.4 in x 0.9 in to fit into X-band waveguide for microwave measurements.

3. Characterization

The products were characterized by X-ray diffraction (XRD), which was conducted on a Rigaku X-ray Diffracrometer, ULTIMA III with Cu Kα radiation (λ=1.5418 Å). Scanning electron microscopy (SEM), it was obtained on a VEGA, TESCAN. Energy-dispersive X-ray spectroscopy (EDX) attached to SEM, while EDX analysis was performed to understand their chemical constituents. Transmission electron microscopy (TEM) was obtained on a JEOL JEM-2100 microscope. The scattering parameters (S_{11} & S_{21}) were measured employing Agilent vector network analyzer (ENA E5071C).

4. Results and Discussion

4.1 Structure Characterization

Fig.-1 show that XRD patterns of $BaTiO_3$ and $BaTiO_3$/NZF composite. The main peak of barium titanate are at 2θ= 22.23º, 31.51º, 38.90º, 45.36º, 51.08º, 56.02º, 56.28º, 65.78º, 70.38º, 75.07º and 79.43º, which exhibit tetragonal perovskite structure. The main peak of NZF are at 2θ= 30.05º, 35.40º, 37.03º, 43.02º, 53.37º, 56.89º, 62.47º and 70.87º, which exhibit the typical spinel structure. Both the XRD patterns of $BaTiO_3$ and NZF are perfectly matched with the reference XRD patterns (JCPDS, PDF no. 04-009-3215 & 01-072-6799 respectively).

Fig.-2(a) & 2(b) represent the SEM images of DBSA-doped PANI and $BaTiO_3$/NZF composite. Fig. - 2(a) showed that the DBSA-doped PANI has smooth surface. The SEM image of $BaTiO_3$/NZF showed that the particles were almost spherical and $BaTiO_3$ & NZF particles were closely associated with each other due to the interaction between dielectric and magnetic phases. Fig. - 2(c), 2(d), 2(e) & 2(f) represent the SEM images of RAM- I, II, III & IV respectively. From Fig. - 2(c) to 2(f), it was shown that the concentration of $BaTiO_3$/NZF composite increases (RAM- I to RAM- IV) and the fillers were uniformly dispersed into the polymeric matrices. Fig.-3(a) & 3(b) show the EDX patterns of DBSA-doped PANI and RAM- II respectively. Nitrogen was not detected in the EDX analysis because the SEM was run with nitrogen gas purging during the analysis and the detector is not standardized to detect Nitrogen. Fig. - 3(a) showed that sulfur (s), oxygen (o), carbon (c) were present in DBSA-doped PANI and Fig.- 3(b) showed that the all components were present in the composites.

Fig. - 4(a) & 4(b) represent the HR-TEM images of DBSA-doped PANI and $BaTiO_3$/NZF composite. From TEM images it was shown that, the particles were almost spherical and particle size was approximately 30nm. Fig. - 4(c) represents the HR-TEM image of RAM- II and showed that the nanoparticles and PANI were uniformly dispersed in the polymeric matrices.

4.2 Microwave Absorbing Properties

From the scattering parameters S_{11} & S_{21}, we have calculated the reflection coefficient (Γ) with the help of the following equations (24)-

$$\Gamma = x \pm \sqrt{(x^2 - 1)}; \quad |\Gamma| \le 1$$

Where x = $(S_{11}^2 - S_{21}^2 + 1)/2S_{11}$

Reflection loss (in dB) = -20log[Γ]

Fig. - 5 represent the measured absorption spectra of RAM- I, II, III & IV. The prepared RAMs showed the absorbing properties in a wide frequency range in the X-band region. RAM- I, II, III & IV showed the maximum reflection loss of -14.86 dB at 10.89 GHz, -13.87 dB at 9.95 GHz, -15.78 dB at 10.89 GHz & -13.43 dB at 10.85 GHz respectively. RAM- I, II, III & IV contain 75%, 50%, 25% & 0% PANI respectively. The content of PANI decreases from RAM- I to IV. RAM- III showed the maximum reflection loss i.e. better absorption than the other RAMs. As the concentration of PANI decrease, the absorbing properties decrease except RAM- III. With increasing the concentration of PANI, the conductivity of the composite materials increase and these contribute to the high permittivity. When the weight ratio of $BaTiO_3$/NZF is 75% (RAM-III), the dielectric properties have

perfectly matched with the magnetic properties. Due to this, RAM-III showed maximum dielectric loss than the other RAMs. For the current composite materials, the dielectric loss is higher than magnetic loss. RAM- I also showed better absorption properties. The mechanism of microwave absorption was clearly described with the help of real and imaginary parts of permittivity and permeability.

4.3 Relative Complex Permittivity and Permeability

To investigate the possible mechanism of microwave absorption, we determined the real and imaginary parts of complex permittivity (ε_r', ε_r'') and permeability (μ_r', μ_r'') from the scattering parameters with the help of Nicolson- Ross- Weir (NRW) method (Paula et al., 2011). Fig. - 6(a) & 6(b) show the real and imaginary parts of complex relative permittivity spectra respectively. Fig.- 6(c) & 6(d) show the real and imaginary parts of complex relative permeability. The real part of permittivity (ε_r') is a measure of how much energy from an external electric field is stored in a material. The imaginary part of permittivity (ε_r'') is known as loss factor and is a measure of how much energy dissipated or lost. The values of real parts of permittivity (ε_r') for RAM-I lie from 3.81 to 5.11. The ε_r' for RAM- II is highest and the values lie from 4 to 5.56. The values of ε_r' for RAM-III lie from 3.54 to 4.91 and for RAM-IV, 3.81 to 4.67 i.e. an increasing trend with increase in frequency. With decrease in PANI concentration, dielectric constant (ε_r') decreases except RAM- II. Orientation polarization and interfacial polarization are the two main contributions for ε_r'. In case of RAM- II, PANI and $BaTiO_3$/NZF are in 1:1 ratio so that the interfacial polarization should be higher. The values of ε_r'' for RAM- I lie from 0.22 at 8.22 GHz to 0.34 at 12.4 GHz and for RAM- II lie from 0.18 to 0.41. The ε_r'' for RAM- III is highest and the values lie from 0.22 to 1.15 i.e. a increasing trend with increasing frequency. The values of ε_r'' for RAM- IV lie from 0.22 to 0.05 i.e. a decreasing trend with increasing frequency. In case of RAM-III, the composites have good compatible dielectric and magnetic properties. The dominant polarization and the conductive losses may be higher for RAM-III. The values of real parts of permeability (μ_r') for RAM- III & I are almost same and values lie from 4.02 to ~3.25. The values of μ_r' for RAM- II & IV lie from 3.79 to 3.09 and 3.47 to 2.93 respectively. The imaginary parts of permeability μ_r'' for all the RAMs are almost zero. From the permittivity and permeability data, it can be concluded that the dielectric loss is more important than magnetic loss.

$BaTiO_3$ has face centered cubic (fcc) structure in which the Ti^{4+} ions have six-fold coordination, surrounded by an octahedron of O^{2-} ions and Ba^{2+} ions have 12-fold cub-octahedral coordination. $BaTiO_3$ has permanent dipoles and it absorbs electrical energy. Nickel-zinc ferrite (NZF) is a typical soft ferromagnetic material. NZF have inverse spinel structure in which Ni^{2+} & half of Fe^{3+} ions occupy the octahedral hole and Zn^{2+} & rest of the Fe^{3+} ions occupy in the tetrahedral hole. Interfacial polarization may occur at the interface between $BaTiO_3$ & NZF. Interfacial polarization may also occur between PANI & $BaTiO_3$ and PANI & NZF. The electric field loss is caused by the dielectric relaxation effect associated with permanent & induced molecular dipoles. An applied electric field creates a torque on electric dipole and the dipole rotate to align with the electric field i.e. orientation polarization occurs. At microwave frequencies i.e. at higher frequencies, the electric field energy changes quickly. There occurs a lack of alignment due to viscosity of the composite material. The friction accompanying the lack of alignment leads to energy dissipation in a form of heat. Magnetic field loss occurs due to hysteresis loss, eddy-current loss and residual loss (Zaag and P.J., 1999). PANI is protonated with DBSA, possesses permanent electric dipoles. Joule-heating loss is occurring due to the finite conductivity of doped PANI. The permanent & dominant polarization and also the associated relaxation phenomenon contribute to the loss mechanism (Abbas et al., 2005). Further, the prepared composites are a heterogeneous mixture in which PANI and $BaTiO_3$/NZF are mixed into the non-conducting epoxy resin matrices. Thus the additional dielectric performance of heterogeneous mixture arises due to interfacial polarization.

5. Conclusions

The composite absorbers based on DBSA-doped PANI and $BaTiO_3$/NZF have been successfully prepared in epoxy resin matrices. XRD, SEM, EDX and HR-TEM have established the formation of composites. The complex relative permittivity, permeability and their relationship with microwave absorption were investigated. It is found that the absorption properties increase with increasing the concentration of PANI. RAM- III has shown maximum reflection loss of -15.78 dB at 10.89 GHz. In RAM- III, the weight ratio of DBSA-doped PANI and $BaTiO_3$/NZF has 1:3. The dominant polarization and the dielectric loss are higher for RAM- III. For the present composites, magnetic losses are less important and dielectric loss and the joule-heating loss has major contribution to the loss mechanism.

References

Abbas, S. M., Dixit, A. K., Chatterjee, R., & Goel, T. C. (2005). Complex permittivity and microwave absorption properties of BaTiO$_3$–polyaniline composite. *Materials Science and Engineering B, 123,* 167-171. http://dx.doi.org/10.1016/j.mseb.2005.07.018

Aphesteguy, J. C., & Jacobo, S. E. (2004). Composite of polyaniline containing iron oxides. *Physica B, 354,* 224–227. http://dx.doi.org/10.1016/j.physb.2004.09.053

Babazadeh, M. (2009). Aqueous Dispersions of DBSA-Doped Polyaniline: One-Pot Preparation, Characterization, and Properties Study. *Journal of Applied Polymer Science*, *113,* 3980-3984. http://dx.doi.org/10.1002/app.30460

Burke, N. A. D., Stover, H. D. H., & Dawson, F. P. (2002). Magnetic Nanocomposites: Preparation and Characterization of Polymer-Coated Iron Nanoparticles. *Chemistry of Materials*, *14,* 4752-4761. http://dx.doi.org/10.1021/cm020126q

Chen, X., Wang, G., Duan, Y, & Liu, S. (2007). Microwave absorption properties of barium titanate / epoxide resin composites. *Journal of Applied Physics*, *40,* 1827-1830.

Fan, Z. G., Luo, G. H., Zhang, Z. G., Zhou, L., & Wei, F. (2006). Electromagnetic and microwave absorbing properties of multi-walled carbon nanotubes/polymer composites. *Materials Science and Engineering B, 132,* 85–89. http://dx.doi.org/10.1016/j.mseb.2006.02.045

Fetisov, Y. K., Bush, A. A., Kamentsev, K. E., & Srinivasan, G. (2004). Pyroelectric effects in magnetoelectric multilayer composites. *Solid State Communications*. *132,* 319-324. http://dx.doi.org/10.1016/j.ssc.2004.07.070

John, D., Washington, M., Aviat. (1988). *Week Space Technol. 129,* 28–29.

Kadam, S. L., Kanamadi, C. M., Patankar, K. K., & Chougule, B. K. (2005). Dielectric behaviour and magnetoelectric effect in Ni $_{0.5}$Co$_{0.5}$Fe $_2$O $_4$+Ba $_{0.8}$Pb$_{0.2}$ Ti O$_3$ ME composites. *Materials Letters*, *59,* 215-219. http://dx.doi.org/10.1016/j.matlet.2004.08.033

Kanai, T., Ohkoshi, S. I., & Nakajima, A. (2001). A Ferroelectric Ferromagnet Composed of (PLZT)x(BiFeO$_3$)$_{1-}$$x$ Solid Solution. *Advanced Materials, 13,* 487-490. http://dx.doi.org/10.1002/1521-4095(200104)13:7%3C487::AID-ADMA487%3E3.0.CO;2-L

Li, L., Jiang, J., & Xu, F. (2007). Synthesis and ferrimagnetic properties of novel Sm-substituted LiNi ferrite polyaniline nanocomposite. *Materials Letters*, 61, 1091–1096. http://dx.doi.org/10.1016/j.matlet.2006.06.061

Li, L., Liu, H., Wang, Y., Jiang, J., & Xu, F. (2008). Preparation and magnetic properties of Zn–Cu–Cr–La ferrite and its nanocomposites with polyaniline. *Journal of Colloid and Interface Science, 321,* 265-271. http://dx.doi.org/10.1016/j.jcis.2008.02.013

Maeda, T., Sugimoto, S., Kagotani, T., Tezuka, N., & Inomata, K. (2004). Effect of the soft/hard exchange interaction on natural resonance frequency and electromagnetic wave absorption of the rare earth–iron–boron compounds. *Journal of Magnetism and Magnetic Materials, 281,* 195-205. http://dx.doi.org/10.1016/j.jmmm.2004.04.105

MacDiarmid, A. G., & Epstein, A. J. (1995). Secondary doping in polyaniline. *Synthetic Metals, 69,* 86-92. http://dx.doi.org/10.1016/0379-6779(94)02374-8

Mathur, R., Sharma, D. R., Vadera, S. R., & Kumar, N. (2001). Doping of emeraldine base with the monovalent bridging iron oxalate ions and their transformation into nanostructured conducting polymer composites. *Acta Materialia*, *49,* 181–187. http://dx.doi.org/10.1016/S1359-6454(00)00220-2

Moghaddam, B., & Nazari, T. (2008). Preparation of Polyaniline/Nanometer-scale Alumina Composite by the Potential Cycling Method. *International Journal of Electrochemical Science, 3,* 768-776

Paula, A. L., Rezende, M. C., & Barroso, J. J. (2011). Experimental measurements and numerical simulation of permittivity and permeability of Teflon in X band. *Journal of Aerospace Technology and Management, 3, 59-64.*

Sarac, S., Ates M., & Kilic, B. (2008). Electrochemical Impedance Spectroscopic Study of Polyaniline on Platinum, Glassy Carbon and Carbon Fiber Microelectrodes. *International Journal of Electrochemical Science*, *3,* 777-786.

Singh, P., Babbar, V. K., Razdan, A., Srivastava, S. L., & Goel, T. C. (2000). Microwave absorption studies of Ca–NiTi hexaferrite composites in X-band. *Materials Science and Engineering B*, *78,* 70-74. http://dx.doi.org/10.1016/S0921-5107(00)00511-0

Soto-Oviedo, M. A., Araú jo, O. A., Faez, R., Rezende, M. C., & De Paoli, M. A. (2006). Antistatic coating and electromagnetic shielding properties of a hybrid material based on polyaniline/organoclay nanocomposite and EPDM rubber. *Synthetic Metals, 156,* 1249-1255. http://dx.doi.org/10.1016/j.synthmet.2006.09.003

Testino, A., Mitoseriu, L., Buscaglia, V., Buscaglia, M. T., Pallecchi, I., Albuquerque, A. S., Calzona, V., Marre, D., Siri, A. S., & Nanni, P. (2006). Preparation of multiferroic composites of $BaTiO_3$–$Ni_{0.5}Zn_{0.5}Fe_2O_4$ ceramics. *Journal of the European Ceramic Society*, *26,* 3031-3036. http://dx.doi.org/10.1016/j.jeurceramsoc.2006.02.022

Ting, T. H., Yu, R. P., & Jau, Y. N. (2011). Synthesis and microwave absorption characteristics of polyaniline/NiZn ferrite composites in 2–40GHz. *Materials Chemistry and Physics*, *126,* 364–368. http://dx.doi.org/10.1016/j.matchemphys.2010.11.011

Wen, H., Cao, M. H., Sun, G. B., Xu, W. G., Wang, D., Zhang, X. Q., & Hu, C. W. (2008). Hierarchical Three-Dimensional Cobalt Phosphate Microarchitectures: Large-Scale Solvothermal Synthesis, Characterization, and Magnetic and Microwave Absorption Properties. *Journal of Physical Chemistry C, 112,* 15948-15955. http://dx.doi.org/10.1021/jp804602b

Wojkiewicz, J. L., Fauveaux, S., & Miane, J. L. (2003). Electromagnetic Shielding Properties of Polyaniline Composites. *Synthetic Metals, 135,* 127-128. http://dx.doi.org/10.1016/S0379-6779(02)00531-3

Zaag, V., P. J. (1999). New views on the dissipation in soft magnetic ferrites. *Journal of Magnetism and Magnetic Materials,* 196-197, 315-319. http://dx.doi.org/10.1016/S0304-8853(98)00732-X

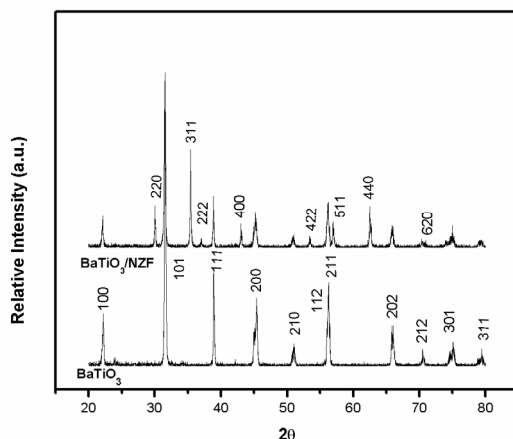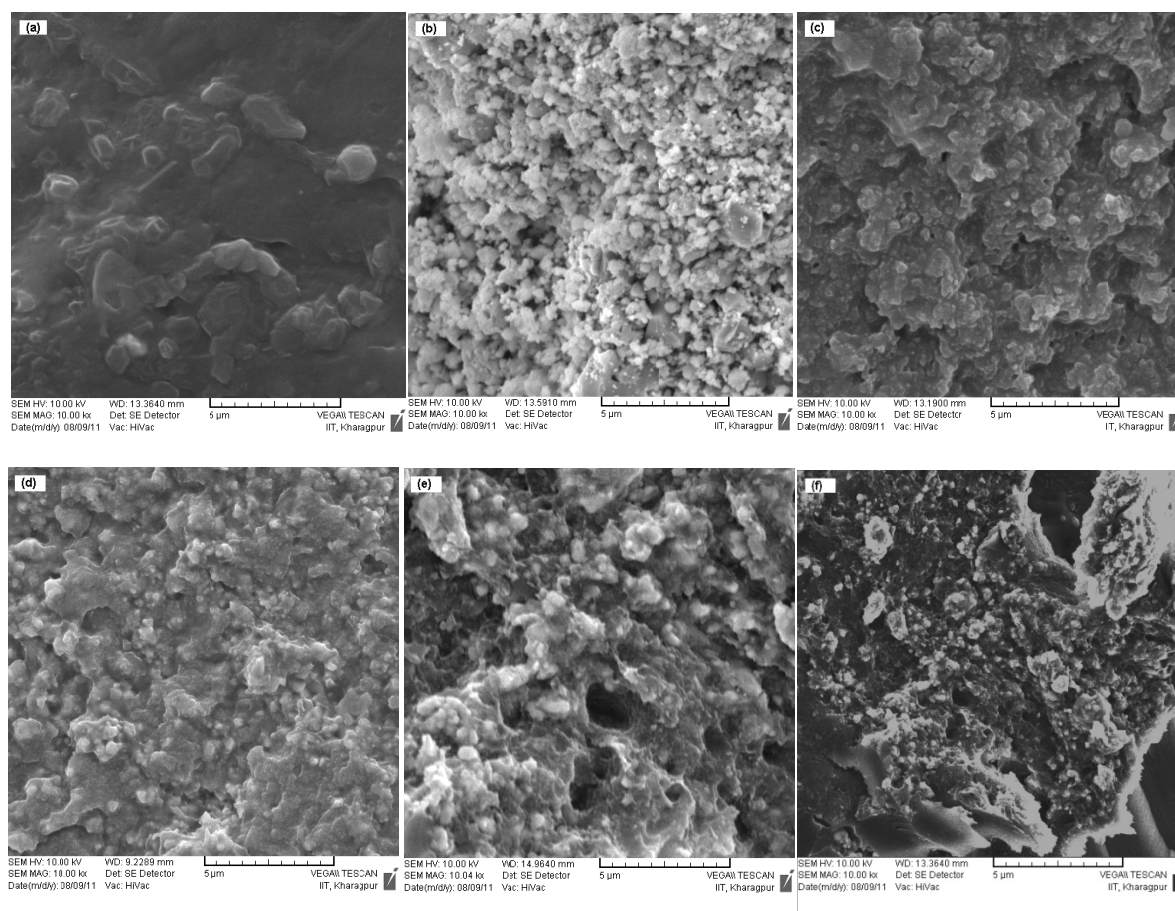Figure 1. XRD patterns of $BaTiO_3$ and $BaTiO_3$/NZF composite

Figure 2. SEM images of (a) DBSA-doped PANI (b) BaTiO$_3$/NZF composite & the fractured cross-section of (c) RAM- I (d) RAM- II (e) RAM- III and (f) RAM- IV
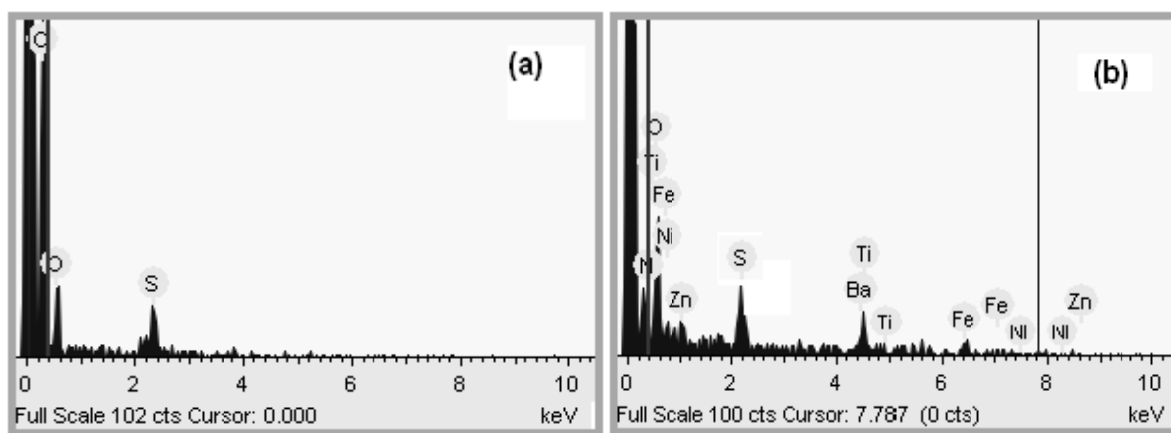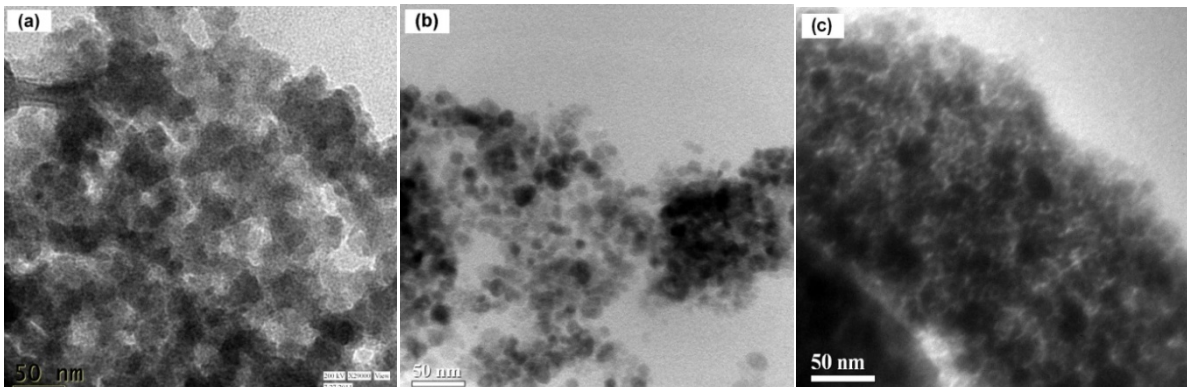

Figure 3. EDX of (a) DBSA-doped PANI (b) RAM- II

Figure 4. HR-TEM images of (a) DBSA-doped PANI (b) BaTiO$_3$/NZF composite (c) RAM-II
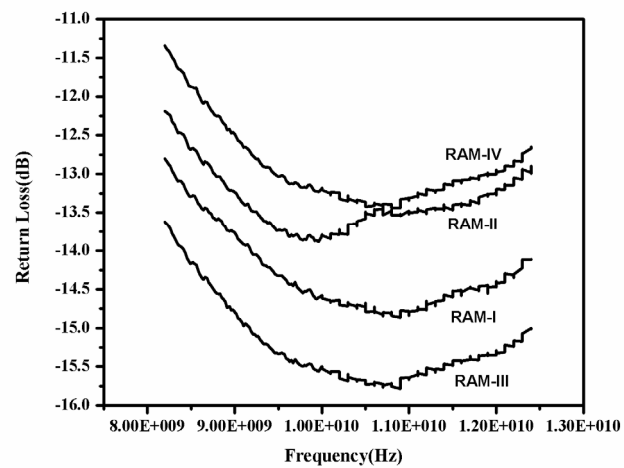

Figure 5. Absorption characteristics of prepared radar absorbing materials at 8.2-12.4 GHz
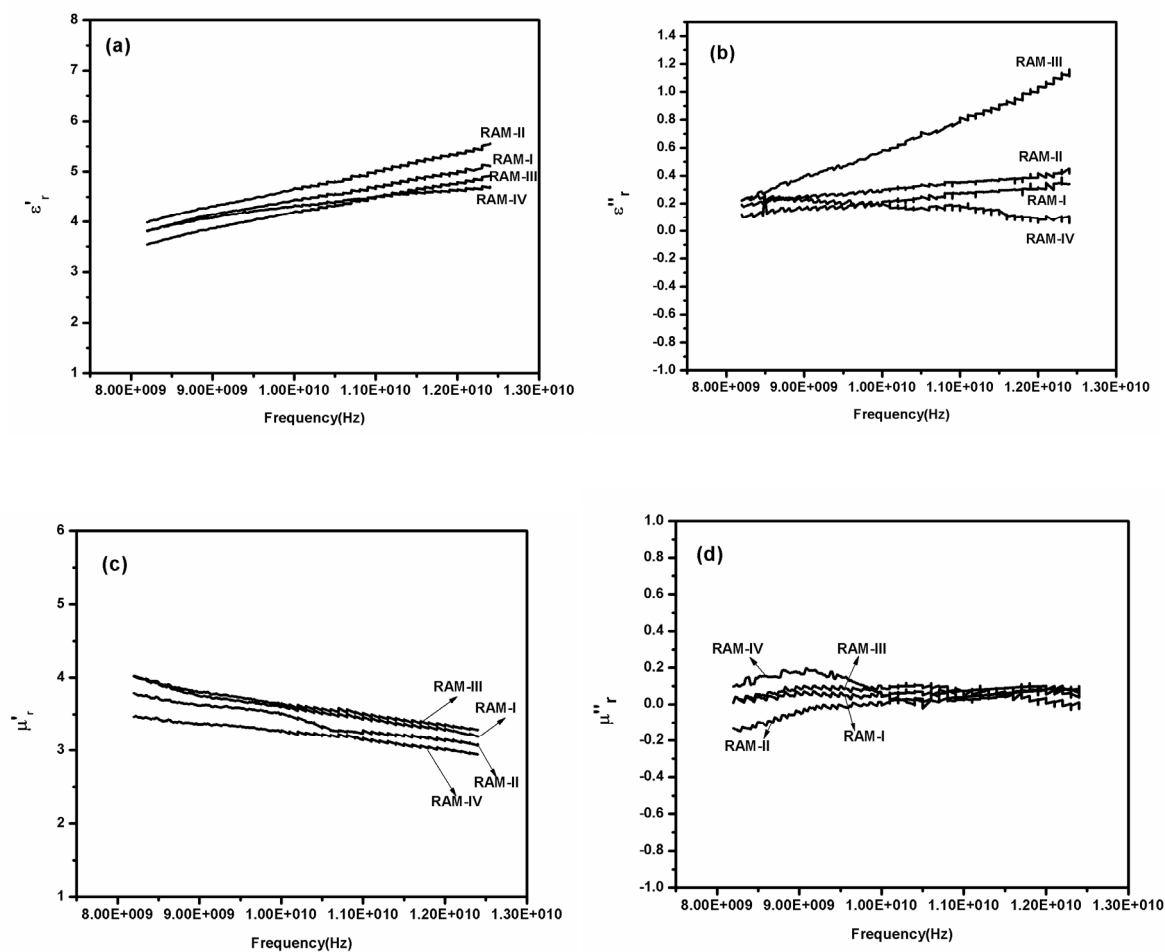
Figure 6. (a) Real (ε_r') and (b) imaginary (ε_r'') parts of relative complex permittivity, (c) real (μ_r') and (d) imaginary (μ_r'') parts of relative complex permeability of prepared RAMs